Research Article

Hierarchical Low Si/Al Ratio Ferrierite Zeolite by Sequential Postsynthesis Treatment: Catalytic Assessment in Dehydration Reaction of Methanol

Enrico Catizzone (ID)**, Massimo Migliori, Alfredo Aloise, Rossella Lamberti, and Girolamo Giordano**

Department of Environmental and Chemical Engineering, University of Calabria, Rende 87036, Italy

Correspondence should be addressed to Enrico Catizzone; enrico.catizzone@unical.it

In contrast to high silica zeolites, it is difficult to obtain mesoporosity in zeolites with low Si/Al ratio (e.g., <20) via conventional NaOH-based treatment, making the obtainment of hierarchical zeolites with high acidity a challenging target. In this paper, we report the preparation of hierarchical FER-type zeolite at low Si/Al molar ratio (about 10) by postsynthesis etching involving a sequence of three treatments with $NaAlO_2$, HCl, and NaOH solutions and investigate the effect of both $NaAlO_2$ solution concentration and time of treatment on the textural properties. The obtained materials exhibit a mesoporous volume higher than the parent ferrierite with no significant effect on the sample acidity. The catalytic activity of some samples was investigated in vapour-phase methanol dehydration to dimethyl ether, revealing the superiority of hierarchical zeolites in terms of methanol conversion, although the presence of mesopores causes formation of light hydrocarbons at high temperatures.

1. Introduction

Zeolites are well-known crystalline aluminosilicates largely applied as catalysts in several industrial processes because of the unique molecular shape selectivity exhibited by these materials due to well-defined regular microporous structure. The possibility to tune the voids system in these materials (openings and spatial orientation of channels, size, and location of cages, etc.) allows to have a catalyst capable of directing the reaction pathway towards formation of desired products [1]. Beside shape selectivity, the acid-base properties of zeolites are of paramount importance in catalysis. Both Brønsted and Lewis acid sites are normally present in zeolites and their concentration, distribution, strength, and location are well-known factors affecting activity, selectivity, and deactivation of the catalyst. Beside these indisputable advantages, zeolites suffer from severe intracrystalline mass transfer limitations due to comparable size of the diffusing molecules and zeolite voids. In zeolites, the diffusing molecules are continuously affected by the interaction with the

channel walls and this type of intracrystalline diffusion is known as configurational diffusion, in order to differentiate it from faster Knudsen-type diffusion. This constrained diffusion in zeolites hinders the reactant molecules to reach the active sites confined in the channels, negatively affecting the catalyst effectiveness. In order to overcome this problem, several strategies can be adopted trying to make more accessible the active sites to the reactant molecules.

As well discussed by Pérez-Ramírez et al. [2, 3], mass transfer limitations inside zeolite crystals can be improved by using zeolites with different porosity levels (e.g., hierarchical porosity) in which the molecular-sized channels are interconnected and connected to the external crystal surface through mesopores facilitating the reactants to access the active sites. During the last decade, several methods to obtain hierarchical micro/mesoporous zeolites are reported following either bottom-up (e.g., carbon-templating) or top-down (e.g., desilication) approaches, showing how hierarchization technique strongly affects physicochemical properties of zeolites (e.g., pore architecture, position, and topology of

mesopores) and the catalytic performances as consequence. The chemical-physical properties of starting materials also play a crucial role in producing hierarchical zeolites. In particular, the efficiency in forming mesoporous surface of conventional NaOH postsynthesis treatment strongly depends on the Si/Al ratio of starting zeolite, showing the highest values in Si/Al range of 25–50. Indeed, for Si/Al < 15, the presence of framework aluminium prevents silicon leaching, limiting mesopores formation; on the other hand, for Si/Al > 200, alkaline treatment causes an excessive and uncontrolled Si extraction resulting in formation of macropores and loss of intrinsic micropore voids [4–6].

Recent works showed that FER-type zeolite can be considered a selective acid catalyst to produce dimethyl ether (DME) via both methanol dehydration and one-pot CO_2 hydrogenation. DME is a reliable alternative fuel for diesel engines due to its high cetane number and soot-free emissions [7, 8]. Moreover, DME can be produced from biomass or CO_2 and, as it can also be used as an intermediate to produce olefins and chemicals, it is considered a promising energetic vector of the future for introducing renewable energy in the chemical industry [9–11]. The valorisation of biomass by using zeolites is receiving a growing attention because it opens new ways for application of these materials in low temperature and liquid phase reactions of biomass or biomass-derived compounds [12, 13]. Compared with other zeolites such as MFI, BEA, EUO, MTW, the 2-D small/medium pore system of FER-type zeolite inhibits the coke formation and offers high DME selectivity during methanol dehydration reaction [14, 15]. In particular, FER-type zeolite with Si/Al = 8–10 exhibits a higher activity and higher TOF than zeolite with higher Si/Al [16]. Furthermore, a recent study showed the superiority of FER-type zeolite over commercial γ-Al_2O_3 (the industrial catalyst of vapour phase methanol-to-DME process), in terms of catalytic resistance in the presence of water, this being a product of reaction that strongly inhibits the activity of γ-Al_2O_3 [17]. The superiority of FER-type zeolite over other zeolites was also reported for one-pot CO/CO_2 hydrogenation to DME process, revealing reliable DME productivity [15–19]. Prasad et al. [18] report that the superiority of ferrierite over other investigated zeolites (i.e., ZSM-5, NaY, and HY) is related to the suitable acid properties as well as a suitable channel topology that retards catalyst deactivation. Similar results were also found by Montesano et al. [19], showing that DME is the main dehydration product obtained during the syngas-to-DME process. Kang et al. [20] and Bae et al. [21] showed that the catalytic behaviour of Cu/ZnO/Al_2O_3-ferrierite systems modified with zirconia exhibit higher stability during the reaction. The high activity of ferrierite-based catalysts was also found for bio-syngas or CO_2 one-pot conversion to DME [22, 23]. In particular, Bonura et al. report that deactivation of ferrierite-based catalyst depends on both acidity and the crystal size of zeolite [24]. Nevertheless, a very little attention has been paid to investigate the catalytic behaviour of hierarchical FER zeolite. The aim of this study is to investigate on the possibility to obtain hierarchical FER-type zeolites, starting from an FER zeolite with a low Si/Al value of 10 and to assess the effect of generated mesopores on catalysis during methanol dehydration to dimethyl ether.

2. Materials and Methods

2.1. Synthesis of Samples. Parent FER-type zeolite was synthesised with a Si/Al value of 10 by using pyrrolidine (Py) as a structure directing agent by adopting the following molar gel composition [25]:

$$SiO_2 - 0.08\,Na_2O - 0.05\,Al_2O_3 - 0.6\,Py - 20\,H_2O \qquad (1)$$

The starting synthesis gel was prepared at room temperature as follows: 0.25 g of NaOH (Aldrich) and 2 g of NaAlO$_2$ (54 wt.% Al_2O_3, Aldrich) were dissolved in 57.1 g of distilled water. Afterwards, 9 g of pyrrolidine (99%, Aldrich) was added, and the system was kept in closed PP bottle under stirring for 30 min, then 31.7 g of colloidal silica (LUDOX AS40, Aldrich) was added in drops, resulting in an opaque gel under vigorous stirring for 1 h. The crystallization was performed in a 100 ml PTFE-lined stainless steel autoclave in a tumbling oven (tumbling speed = 25 rpm) kept at 180°C for 3 days. After synthesis, the autoclave was quenched in cold water and the solid was recovered by suction filtration followed by careful washing with distilled water. Organic SDA was removed by calcination in static air at 550°C for 8 h, and after this treatment, the H-form of the synthesised zeolites was prepared by a double ion-exchange with 1 M NH$_4$Cl solution (100 ml/g$_{zeolite}$) at 80°C, followed by calcination in static air at 550°C for 8 h.

Hierarchical FER-type zeolites were prepared on the basis of the method proposed by Verboekend et al. [26]. The H-form parent FER powder was subjected to consecutive treatments with NaAlO$_2$, HCl, and NaOH solutions. In the first step, about 1 g of parent zeolite was treated with NaAlO$_2$ (10 ml$_{sol}$/g$_{zeolite}$) at 80°C in a closed PP bottle under vigorous stirring. The effect of both concentration and contact time was investigated by using 1 M, 1.5 M, and 2 M NaAlO$_2$ solutions for 0.5, 1.5, and 3 h; afterwards, the solution was quenched in an ice-water bath. According to Verboekend et al. [26], the secondary step consists of removing extra-framework aluminium species by treating the solid with a 3 M HCl solution (10 ml$_{sol}$/g$_{zeolite}$) under stirring at 80°C. Finally, the third step consists of an alkaline treatment with a 0.2 M NaOH solution (30 ml/g$_{zeolite}$) under stirring at 60°C for 30 min in order to remove silicon-rich debris. After each step, the solid was recovered by filtration, washed with distilled water until neutral pH, and dried overnight. The resulting solid was then transformed to protonic form by the same procedure reported for the parent sample. Table 1 reports the treatment conditions adopted in this work.

2.2. Characterization. Powered X-ray diffraction patterns of synthesised samples were obtained with APD 2000 Pro GNR instrument (Cu Kα radiation, λ = 1.5406, 40 kV, 30 mA, 5–50° 2θ range, scanning step 0.2°·s^{-1}). Crystal habit was observed via scanning electron microscopy (FEI model Inspect). Nitrogen isotherms adsorption/desorption

TABLE 1: List of investigated samples. All treated samples underwent trough step 2 and step 3.

Sample	Description of postsynthesis treatment
P	Parent sample, untreated
A1	Treated with 1 M $NaAlO_2$ for 0.5 h
B1	Treated with 1 M $NaAlO_2$ for 1.5 h
C1	Treated with 1 M $NaAlO_2$ for 3 h
D1	Treated with 1 M $NaAlO_2$ for 6 h
C1.5	Treated with 1.5 M $NaAlO_2$ for 3 h
B2	Treated with 2 M $NaAlO_2$ for 1.5 h
C2	Treated with 2 M $NaAlO_2$ for 3 h
DesNaOH	Treated with 0.2 NaOH at 80°C for 6 h

measurements were carried out at −196°C with Micromeritics ASAP 2020 instrument, following the procedure discussed elsewhere. For comparative purpose with published studies on hierarchical ferrierite zeolites [27–31], specific surface area was estimated from Brunauer-Emmett-Teller (BET) equation whilst both micropore volume and external surface were calculated by the t-plot method, adopting the Harkins–Jura as the master isotherm [32–36], although such methods may have some limitation for micro/mesoporous materials [37]. Pore size distribution was obtained by applying the Barrett–Joyner–Halenda (BJH) to the adsorption branch of the isotherms. Chemical composition of the investigated samples was determined via atomic absorption spectroscopy (GBC 932). Surface acidity was assessed by temperature programmed desorption of ammonia (NH_3-TPD) measurements with a TPDRO1100 (ThermoFisher) equipped with a thermal conductivity detector (TCD), according to the following procedure. Dried sample (100 mg, powder form) was loaded in a linear quartz microreactor and pretreated at 300°C in helium flow (20 STP ml·min^{-1}, STP referred at 0°C and 1 bar) for 1 h to remove the adsorbed water. The sample was cooled down to 150°C and saturated with 10% v/v NH_3/He mixture with a flow rate of 20 STP ml·min^{-1} for 2 h. Ammonia physically adsorbed was removed by purging in helium at 150°C for 1 h until TCD baseline stabilization. Desorption measurement was carried out in the temperature range of 100–550°C (10°C·min^{-1}) using a helium flow rate of 20 STP ml·min^{-1}.

2.3. Catalytic Tests. Vapour-phase methanol dehydration was used to assess the effect of hierarchical pore structure on catalytic behaviour of ferrierite samples. Catalytic tests were carried out in a continuous packed bed quartz reactor loaded with about 70 mg of dried sample. Before feeding methanol, the catalyst was treated under nitrogen flow at 250°C for 2 h in order to remove residual moisture. After setting the reactor temperature to the desired set point, a mixture of methanol (0.06 mol/mol) and nitrogen as a carrier (60 STP ml/min) was fed to the reactor at the weight hourly space velocity (WHSV) of 4.5 $g_{MeOH}/(g_{cat}·h)$. The reactor outstream was analyzed by GC (Agilent 7890 A) equipped with a capillary column (J&W 125−1032) and a FID detector. The detector was kept at 250°C whilst the column was

heated from 40°C to 150°C with a ramp of 10°C using hydrogen as carrier with a constant flow of 8 STP ml·min^{-1}.

3. Results and Discussion

3.1. Physical-Chemical Characterization. Figure 1 shows the XRD patterns in the 2 theta range 20–30° of parent zeolite and the treated samples with 1 M and 2 M $NaAlO_2$ solution for 6 h and 3 h in acid form, respectively. XRD shows that no significant phase change occurs after treatments, even though a little decrease in intensity can be observed.

Table 2 reports the relative crystallinity of investigated samples calculated considering the sum of intensity of peaks at 22.3°, 22.6°, 23.6°, 25.3°, and 25.6° and taking the parent zeolite as reference.

Table 2 shows that crystallinity decreases by increasing both $NaAlO_2$ concentration and treatment time. Samples after 3 h of treatment with $NaAlO_2$ (e.g., C1, C1.5, and C2) show a crystallinity of 91%, 85%, and 79% when the concentration of $NaAlO_2$ solution was 1 M, 1.5 M, and 2 M, respectively. Similarly, by increasing the treatment time the sample shows a lower crystallinity.

Furthermore, after postsynthesis treatments, a shift of reflections towards the lower angle is observes, suggesting some modification of unit cell parameters. Assuming an orthorhombic configuration, the unit cell volume is 1943 Å^3, 1953 Å^3, and 1947 Å^3 for P, D1, and C2 sample, respectively, indicating a negligible change of zeolite lattice after treatment.

Nitrogen adsorption isotherms reported in Figures 2(a) and 2(b) confirm the microporous structure of parent ferrierite sample. On the contrary, for treated samples the nitrogen uptake at a middle-high relative pressure significantly increases by increasing ether contact time (Figure 2(a)) or $NaAlO_2$ concentration (Figure 2(b)). The introduction of additional mesopores after treatment is also highlighted by BJH pore size distribution reported in Figure 3. In particular, by increasing the contact time and $NaAlO_2$, the mesopore volume increases significantly in the range 2–50 nm even if no centered mesoporosity is observed. Similar results were observed also by Verboekend et al. [26], for FER zeolite with Si/Al = 27 after similar treatments. Figure 4 shows a comparison between N_2 isotherms and BJH PSD of parent ferrierite and DesNaOH sample revealing that the treatment with NaOH is less effective in terms of mesopore generation than the combined $NaAlO_2$ + HCl + NaOH sequential method [26].

Table 3 reports both chemical and textural properties of investigated zeolites. Chemical analysis reveals that the hierarchization technique does not significantly affect the Si/Al ratio that is kept in the range 10–12 and only a small reduction of silicon content is found for the sample treated with NaOH. The postsynthesis treatment strongly affects the textural properties of investigated ferrierite as reported in Table 3. The mesopore surface increases as function of both treatment time and $NaAlO_2$ concentration, preserving the micropore volume in the range 0.11–0.13 cm^3/g.

With the aim to have more information on the effect of each treatment, Table 4 reports the main physicochemical

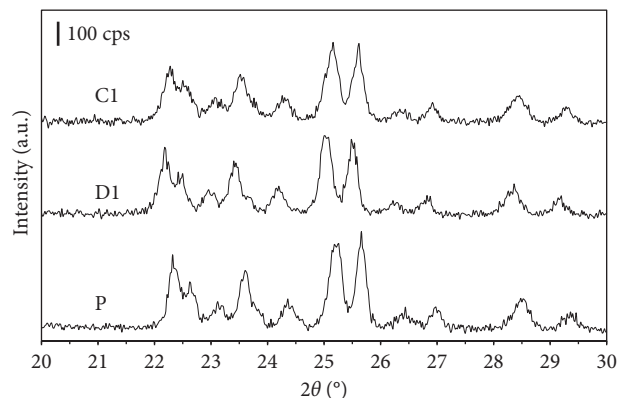Figure 1: XRD pattern in the 2 Theta range 20–30° of parent (P), treated with $NaAlO_2$ 1 M for 6 h (D1) and with $NaAlO_2$ 2 M for 3 h (C2).

Table 2: Relative crystallinity of investigated samples.

Sample	Relative crystallinity (%)
P	100
A1	97
B1	95
C1	91
D1	89
C1.5	85
B2	84
C2	79
DesNaOH	98

properties of each step to produce the D1 sample. In particular, the Si/Al ratio strongly reduces after treatment with $NaAlO_2$ solution, indicating the precipitation of aluminate species on zeolite crystals. This causes a strong reduction of micropore volume and crystallinity of materials (Figure 5). After HCl washing, both crystallinity and microporosity are recovered due to etching of aluminium species. The subsequent alkaline treatment allows to improve crystallinity and to restore the initial Si/Al ratio. After ion-exchange with NH4Cl solution (pH = 5.5), the crystallinity of the sample was further improved.

The results indicate that the applied method is suitable to obtain hierarchical ferrierite with no significant change in microporosity, which is a key point to preserve the shape selectivity of zeolites. The highest increment in mesoporous surface areas and mesoporous volume was obtained for D1 and C2 samples, respectively; therefore, further characterization and catalytic tests were carried out for these samples.

The NH_3-TPD profiles are reported in Figure 6 for parent, D1, and C2 samples displaying two main bands characterized by different ammonia maximum desorption temperature peaks (T_M) as indicator of different acid sites family (the higher is T_M, the stronger is the acid sites).

As suggested by Niwa and Katada [38], the interpretation of peak with $T_M < 300°C$ may be quite misleading because the desorption effect may also be related to physically adsorbed ammonia hydrogen bonded to NH_4^+ ions generated by ammonia effectively adsorbed onto acid sites.

In this condition, having comparable desorption energy, the presence of weak acid sites, may be partially hidden by physisorbed ammonia. On the contrary, the peaks having $300°C < T_M < 500°C$ are associated with ammonia molecules desorbed from medium-strong acid sites (both Brønsted and Lewis acid sites). Quantitative results of NH_3-TPD measurements reported in Table 5 reveal that postsynthesis treatment does not significantly affect neither the total amount nor the weak/strong distribution of acid sites, since all the samples disclose similar acidic properties. The total acidity calculated from NH_3-TPD measurements is lower than that theoretically calculated from aluminium content measured by chemical analysis (about $1500 \, \mu mol/g$ for P and D1 and about $1400 \, \mu mol/g$) indicating that about 30% of aluminium is not acidic or is not accessible for ammonia titration.

3.2. Catalytic Tests. The catalytic activity of synthesised samples was investigated by performing methanol-to-dimethyl ether reaction. Figure 7 shows the methanol conversion as a function of reaction temperature. The reported data are the average value over three independent measurements during 30 min of time-on-stream, always resulting in conversion relative variation below 10%.

Catalytic results clearly show that hierarchical zeolites are more active than parent zeolite, mainly at lower temperatures. For temperatures higher than 220°C, all the catalysts exhibit a similar methanol conversion level approaching the equilibrium value at 240°C. In order to take into account the effect of acidity on catalytic activity, the apparent turnover frequency (TOF_{app}) can be calculated by considering the acid sites concentration measured by NH_3-TPD. At 180°C, the apparent TOF_{app} is 90, 167, and $229 \, h^{-1}$ for P, D1, and C2 samples, clearly indicating the beneficial role of increase of both area and volume of mesopores on accessibility of acid sites and then on catalytic activity. Only DME is observed in the reactor out-stream up to 240°C whilst, at higher temperatures, other hydrocarbons, mainly methane, ethene, and propene are formed. At 280°C, although similar conversion level is achieved from each sample, the DME selectivity is 0.98, 0.96, and 0.94 for P, D1, and C2 samples, respectively, indicating that the presence of mesopores may be responsible for shape selectivity loss and a more rapid formation of intermediates for light hydrocarbon production [39–42].

Figure 8 reports the by-products distribution after 5 min reaction at 280°C, clearly showing that C2 sample exhibits a marked tendency to form propene, whilst P and D1 samples show a similar distribution without any significant difference between small hydrocarbons. During 5 h reaction, no conversion loss was observed for all the samples, whilst DME selectivity progressively approaches the unity, probably due to coke deposition partially deactivating the strong acid sites that are mainly responsible for methanol-to-hydrocarbon conversion.

In order to assess the coke deposition, after 5 h reaction at 280°C the samples were subjected to thermogravimetric analysis by following a procedure detailed elsewhere [42].
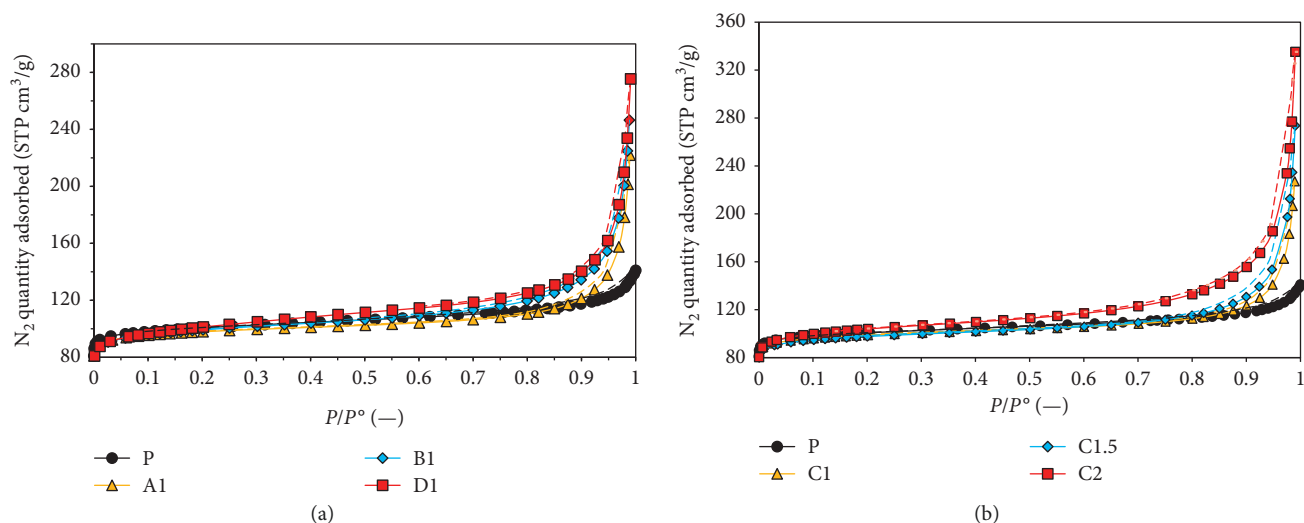
FIGURE 2: N_2 adsorption isotherms at $-196°C$ of parent (P) and samples treated with 1 M $NaAlO_2$ solution at different contact time (A1 = 0.5 h, B1 = 1.5 h, and D1 = 6 h) (a) and $NaAlO_2$ concentration (C1 = 1 M, C1.5 = 1.5 M, and C2 = 2 M) after 3 h treatment (b).
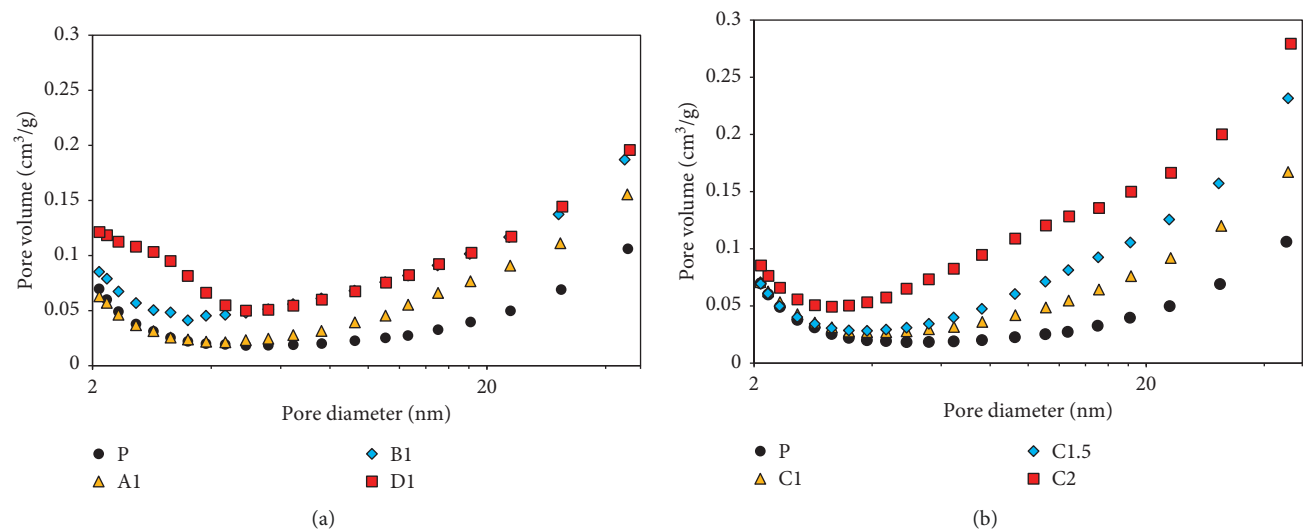

FIGURE 3: BJH pore size distribution derived from N_2 adsorption isotherms of parent (P) and samples treated with 1 M $NaAlO_2$ solution at different contact time (A1 = 0.5 h, B1 = 1.5 h, and D1 = 6 h) (a) and $NaAlO_2$ concentration (C1 = 1 M, C1.5 = 1.5 M, and C2 = 2 M) after 3 h treatment (b).

The results of TGA show that the coke deposited during the reaction was 40 mg/g, 37 mg/g, and 41 mg/g for P, D1, and C2 samples, indicating no significant effect of textural properties on coke deposition under the investigated conditions.

4. Conclusions

The preparation of hierarchical zeolite by desilication starting from zeolites with low Si/Al is a challenge faced in this work. A sequence of postsynthesis modification of ferrierite zeolite with Si/Al = 10 was carried out. The method consists of three steps:

Step 1. Treatment with $NaAlO_2$ solution at 80°C.

Step 2. Treatment with 3 M HCl solution at 80°C.

Step 3. Treatment with 0.2 M NaOH solution at 60°C.

The effect of both $NaAlO_2$ concentration and duration of step 1 on textural properties was assessed. Porosimetry analysis clearly shows that both surface area and volume of mesopores can be increased by increasing both $NaAlO_2$ molarity and treatment time. On the contrary, alkaline treatment with NaOH does not significantly increase mesoporosity of investigated ferrierite. Although there is a significant change in textural properties, both Si/Al and acidity were preserved during the treatment. Methanol dehydration to DME reaction was used as a "probe reaction" aiming to assess the effect of mesopores on accessibility
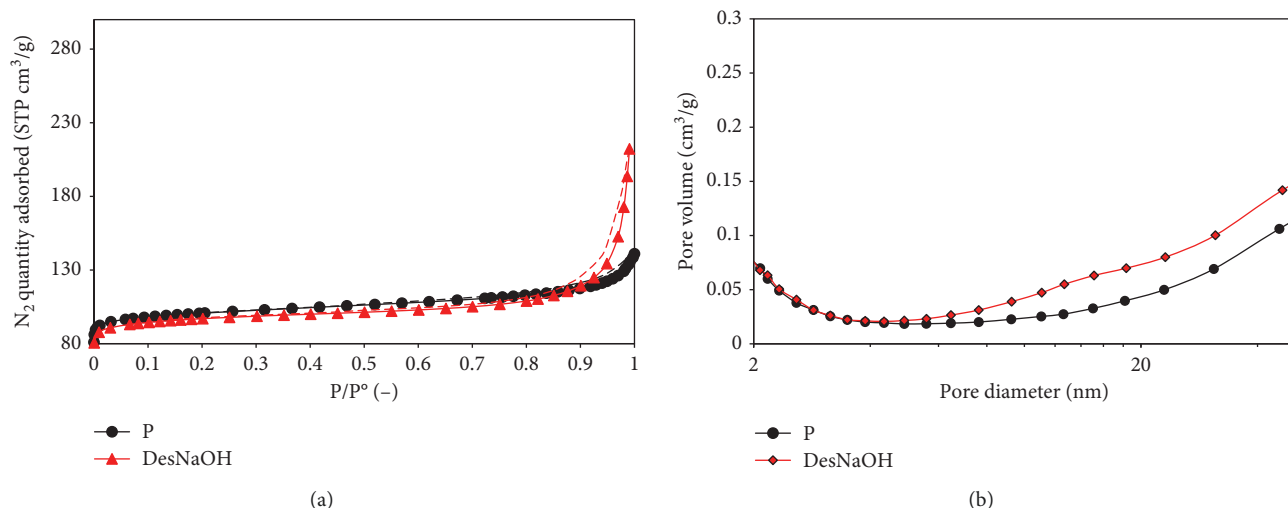
(a)

(b)

FIGURE 4: Effect of NaOH treatment (0.2 M, 6 h, 80°C) on N_2 adsorption isotherms and BJH pore size distribution.

TABLE 3: Chemical and textural properties of investigated samples.

Sample	Si/Al[a] (mol/mol)	V_{pore}[b] (cm^3/g)	V_{micro}[c] (cm^3/g)	S_{BET}[d] (m^2/g)	S_{meso}[c] (m^2/g)
P	10	0.21	0.13	329	50
A1	11	0.24	0.13	329	54
B1	12	0.25	0.12	332	59
C1	12	0.28	0.12	335	75
D1	10	0.29	0.11	342	100
C1.5	11	0.31	0.12	330	65
B2	10	0.32	0.13	349	74
C2	11	0.36	0.12	352	89
DesNaOH	9	0.24	0.13	325	54

[a]Atomic absorption spectroscopy. Average value over three independent measurements with a coefficient of variation below 0.5%. [b]Volume adsorbed at P/P° = 0.99. [c]Micropore volume (V_{micro}) and mesoporous surface area S_{meso} by t-plot with a coefficient of variation below 2%. [d]Total surface area by Brunauer–Emmett–Teller's method with a coefficient of variation below 3%.

TABLE 4: Chemical and textural properties of investigated samples.

Sample	Si/Al[a] (mol/mol)	V_{pore}[b] (cm^3/g)	V_{micro}[c] (cm^3/g)	S_{BET}[d] (m^2/g)	S_{meso}[c] (m^2/g)
Parent	10	0.21	0.13	329	50
SA	5	0.52	0.04	324	230
SA-HCl	15	0.26	0.12	330	71
SA-HCl-NaOH	11	0.28	0.10	338	100
D1	10	0.29	0.12	342	100

[a]Atomic absorption spectroscopy. [b]Volume adsorbed at P/P° = 0.99. [c]Micropore volume (V_{micro}) and mesoporous surface area S_{meso} by t-plot. [d]Total surface area by Brunauer–Emmett–Teller's method.
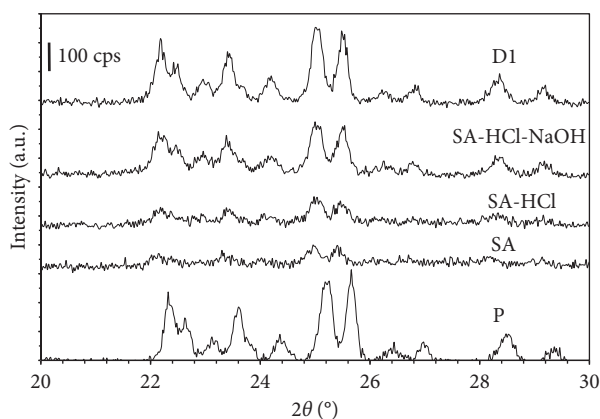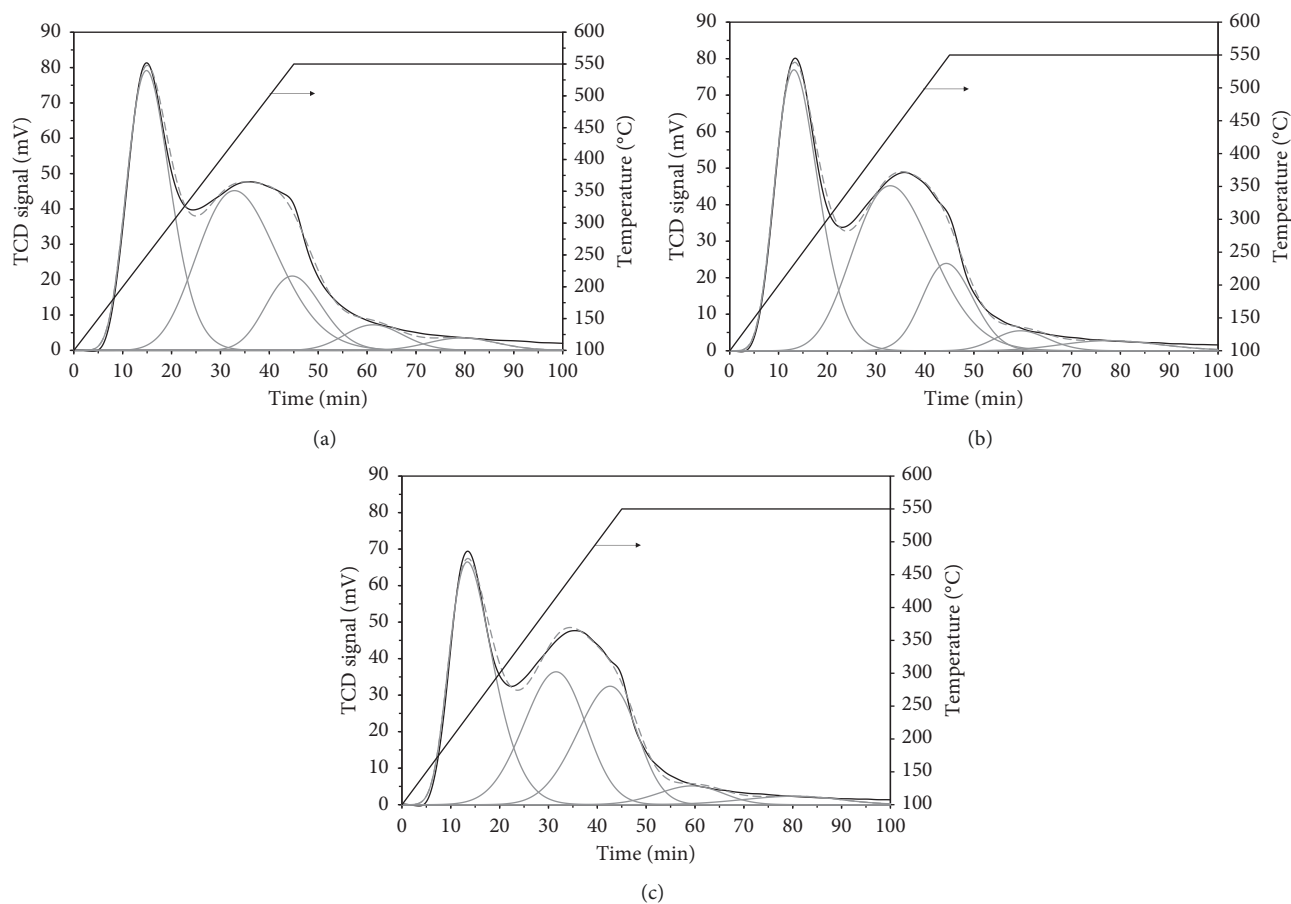

FIGURE 5: XRD patterns of parent and treated ferrierite sample. SA: after treatment with $NaAlO_2$ 1 M for 6 h; SA-HCl: SA sample treated with HCl solution; SA-HCl-NaOH: SA-HCl sample treated with NaOH solution. More details in the experimental part.

(a)

(b)

(c)

FIGURE 6: NH₃-TPD profiles of parent (a), D1 (b), and C2 (c) samples.

TABLE 5: Results of NH₃-TPD measurements.

Sample	NH$_3$ uptake (μmol/g$_{cat}$)	$T_{M,LT}$[a] (°C)	x_{LT}[b]	$T_{M,HT}$[c] (°C)	x_{HT}[d]
P	1178	239	0.39	460	0.61
D1	1128	234	0.39	458	0.61
C2	1025	234	0.38	454	0.62

[a]Temperature of maximum desorption of NH$_3$ between 100 and 300°C. [b]Fractional population of sites between 100 and 300°C. [c]Temperature of maximum desorption of NH$_3$ above 300°C. [d]Fractional population of sites above 300°C.
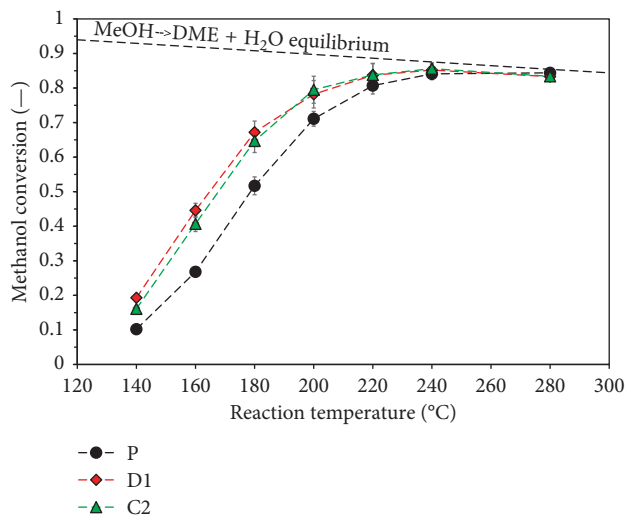

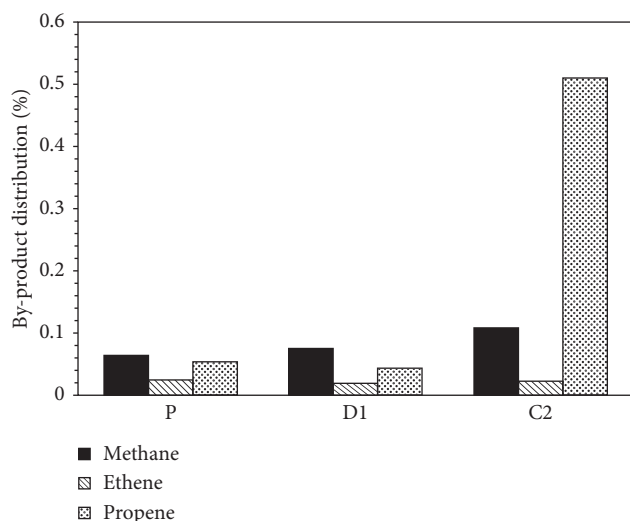FIGURE 7: Methanol conversion as a function of temperature.

Figure 8: By-products distribution during methanol conversion at 280°C after 5 min reaction.

of acid sites. Critical data show that hierarchical zeolites exhibit a higher activity in terms of methanol conversion. On the contrary, the presence of mesopores causes a drop selectivity at 280°C, where hydrocarbons (mainly propene) are formed.

Data Availability

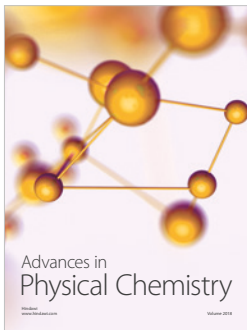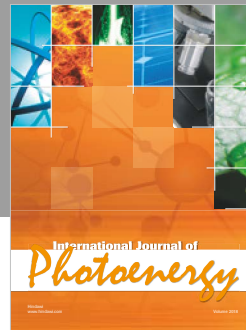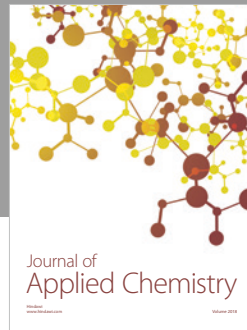The experimental data used to support the findings of this study are included within the article.
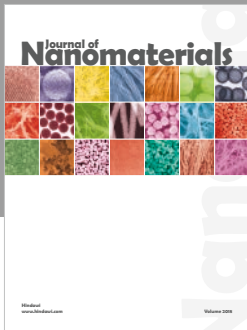
Conflicts of Interest

The authors declare that there are no conflicts of interest regarding the publication of this paper.

References

[1] A. Corma, "State of the art and future challenges of zeolites as catalysts," *Journal of Catalysis*, vol. 216, no. 1-2, pp. 298–312, 2003.

[2] J. Pérez-Ramírez, C. H. Christensen, K. Egeblad, C. H. Christensen, and J. C. Groen, "Hierarchical zeolites: enhanced utilization of microporous crystals in catalysis by advances in materials design," *Chemical Society Review*, vol. 37, no. 11, pp. 2530–2542, 2008.

[3] S. Mitchell, A. B. Pinar, J. Kenvin, P. Crivelli, J. Karger, and J. Pérez-Ramírez, "Structural analysis of hierarchically organized zeolites," *Nature Communications*, vol. 6, no. 1, pp. 1–14, 2015.

[4] J. C. Groen, J. C. Jansen, J. A. Moulijn, and J. Pérez-Ramírez, "Optimal aluminum-assisted mesoporosity development in MFI zeolites by desilication," *Journal of Physical Chemistry B*, vol. 108, no. 35, pp. 13062–13065, 2004.

[5] F. Tian, Y. Wu, Q. Shen, X. Li, Y. Chen, and C. Meng, "Effect of Si/Al ratio on mesopore formation for zeolite beta via NaOH treatment and the catalytic performance in α-pinene isomerization and benzoylation of naphthalene," *Microporous and Mesoporous Materials*, vol. 173, pp. 129–138, 2013.

[6] Z. L. Hua, J. Zhou, and J. L. Shi, "Recent advances in hierarchically structured zeolites: synthesis and material performances," *Chemical Communications*, vol. 47, no. 38, pp. 10536–10547, 2011.

[7] T. A. Semelsberger, R. L. Borup, and H. L. Greene, "Dimethyl ether (DME) as an alternative fuel," *Journal of Power Sources*, vol. 156, no. 2, pp. 497–511, 2006.

[8] C. Arcoumanis, C. Bae, R. Crookes, and E. Kinoshita, "The potential of di-methyl ether (DME) as an alternative fuel for compression-ignition engines: a review," *Fuel*, vol. 87, no. 7, pp. 1014–1030, 2008.

[9] E. Catizzone, G. Bonura, M. Migliori, F. Frusteri, and G. Giordano, "CO_2 recycling to dimethyl ether: state-of-the-art and perspectives," *Molecules*, vol. 23, no. 1, p. 31, 2017.

[10] L. Petrus and M. A. Noordermeer, "Biomass to biofuels, a chemical perspective," *Green Chemistry*, vol. 8, no. 10, pp. 861–867, 2006.

[11] A. Molino, M. Migliori, D. Macrì et al., "Glucose gasification in super-critical water conditions for both syngas production and green chemicals with a continuous process," *Renewable Energy*, vol. 91, pp. 451–455, 2016.

[12] P. Lanzafame, K. Barbera, G. Papanikolaou et al., "Comparison of H + and NH 4 + forms of zeolites as acid catalysts for HMF etherification," *Catalysis Today*, vol. 304, pp. 97–102, 2018.

[13] P. Lanzafame, K. Barbera, S. Perathoner et al., "The role of acid sites induced by defects in the etherification of HMF on Silicalite-1 catalysts," *Journal of Catalysis*, vol. 330, pp. 558–568, 2015.

[14] E. Catizzone, A. Aloise, M. Migliori, and G. Giordano, "From 1-D to 3-D zeolite structures: performance assessment in catalysis of vapour-phase methanol dehydration to DME," *Microporous and Mesoporous Materials*, vol. 243, pp. 102–111, 2017.

[15] E. Catizzone, A. Aloise, M. Migliori, and G. Giordano, "Dimethyl ether synthesis via methanol dehydration: effect of zeolite structure," *Applied Catalysis A: General*, vol. 502, pp. 215–220, 2015.

[16] E. Catizzone, A. Aloise, M. Migliori, and G. Giordano, "The effect of FER zeolite acid sites in methanol-to-dimethyl-ether catalytic dehydration," *Journal of Energy Chemistry*, vol. 26, no. 3, pp. 406–415, 2017.

[17] E. Catizzone, M. Migliori, A. Purita, and G. Giordano, "Ferrierite vs. γ-Al_2O_3: the superiority of zeolites in terms of water-resistance in vapour-phase dehydration of methanol to dimethyl ether," *Journal of Energy Chemistry*, 2018, In press.

[18] P. S. S. Prasad, J. W. Bae, S. H. Kang, Y. J. Lee, and K. W. Jun, "Single-step synthesis of DME from syngas on Cu-ZnO-Al_2O_3/zeolite bifunctional catalysts: the superiority of ferrierite over the other zeolites," *Fuel Process Technology*, vol. 89, no. 12, pp. 1281–1286, 2008.

[19] R. Montesano, A. Narvaez, and D. Chadwick, "Shape-selectivity effects in syngas-to-dimethyl ether conversion over Cu/ZnO/Al_2O_3 and zeolite mixtures: carbon deposition and by-product formation," *Applied Catalysis A: General*, vol. 482, pp. 69–77, 2014.

[20] S. H. Kang, J. W. Bae, K. W. Jun, and H. S. Potdar, "Dimethyl ether synthesis from syngas over the composite catalysts of Cu-ZnO-Al_2O_3/Zr-modified zeolites," *Catalysis Communications*, vol. 9, no. 10, pp. 2035–2039, 2008.

[21] J. W. Bae, S. H. Kang, Y. J. Lee, and K. W. Jun, "Synthesis of DME from syngas on the bifunctional Cu-ZnO-Al_2O_3/Zr-modified ferrierite: effect of Zr content," *Applied Catalysis B: Environmental*, vol. 90, no. 3-4, pp. 426–435, 2009.

[22] J. W. Jung, Y. J. Lee, S. H. Um et al., "Effect of copper surface area and acidic sites to intrinsic catalytic activity for dimethyl ether synthesis from biomass-derived syngas," *Applied Catalysis B: Environmental*, vol. 126, pp. 1–8, 2012.

[23] G. Bonura, C. Cannilla, L. Frusteri, and F. Frusteri, "The influence of different promoter oxides on the functionality of hybrid CuZn-ferrierite systems for the production of DME from CO_2-H_2 mixtures," *Applied Catalysis A: General*, vol. 544, pp. 21–29, 2017.

[24] G. Bonura, M. Migliori, L. Frusteri et al., "Acidity control of zeolite functionality on activity and stability of hybrid catalysts during DME production via CO_2 hydrogenation," *Journal of CO2 Utilization*, vol. 24, pp. 398–406, 2018.

[25] X. Chen, T. Todorova, A. Vimont et al., "In situ and post-synthesis control of physicochemical properties of FER-type crystals," *Microporous and Mesoporous Materials*, vol. 200, pp. 334–342, 2014.

[26] D. Verboekend, R. Caicedo-Realpe, A. Bonilla, M. Santiago, and J. Pérez-Ramírez, "Properties and functions of hierarchical ferrierite zeolites obtained by sequential post-synthesis treatments," *Chemistry of Materials*, vol. 22, no. 16, pp. 4679–4689, 2010.

[27] W. Cu, X. Li, X. Zhu et al., "Size-controlled synthesis of hierarchical ferrierite zeolite and its catalytic application in 1-butene skeletal isomerization," *Microporous and Mesoporous Material*, vol. 240, pp. 189–196, 2017.

[28] K. Brylewska, K. A. Tarach, W. Mozgawa, Z. Olejniczak, U. Filek, and K. Góra-Marek, "Modification of ferrierite through post-synthesis treatments. Acidic and catalytic properties," *Journal of Molecular Structure*, vol. 1126, pp. 147–153, 2016.

[29] P. Wuamprakhon, C. Wattanakit, C. Warakulwit et al., "Direct synthesis of hierarchical ferrierite nanosheet assemblies via an organosilane template approach and determination of their catalytic activity," *Microporous and Mesoporous Materials*, vol. 219, pp. 1–9, 2016.

[30] A. Bonilla, D. Baudouin, and J. Pérez-Ramírez, "Desilication of ferrierite zeolite for porosity generation and improved effectiveness in polyethylene pyrolysis," *Journal of Catalysis*, vol. 265, no. 2, pp. 170–180, 2009.

[31] Y. P. Khitev, Y. G. Kolyagin, I. I. Ivanova et al., "Synthesis and catalytic properties of hierarchical micro/mesoporous materials based on FER zeolite," *Microporous and Mesoporous Materials*, vol. 146, no. 1–3, pp. 201–207, 2011.

[32] P. Hudec, A. Smiešková, Z. idek, P. Schneider, and O. Ŝolcová, "Determination of microporous structure of zeolites by t-plot method-State-of-the-art," *Studies in Surface Science and Catalysis*, vol. 142, pp. 1587–1594, 2002.

[33] S. Lowell, J. E. Shields, M. A. Thomas, and M. Thommes, *Caratcterization of Porous Solids and Powders: Surface Area, Pore Size and Density*, Springer, Berlin, Germany, 2004.

[34] G. Leofanti, M. Padovan, G. Tozzola, and B. Venturelli, "Surface area and pore texture of catalysts," *Catalysis Today*, vol. 41, no. 1–3, pp. 207–219, 1998.

[35] M. Johnson, "Estimation of the zeolite content of a catalyst from nitrogen adsorption isotherms," *Journal of Catalysis*, vol. 52, no. 3, pp. 425–431, 1978.

[36] N. Ayawei, A. N. Ebelegi, and D. Wankasi, "Modelling and interpretation of adsorption isotherms"," *Journal of Chemistry*, vol. 2017, Article ID 3039817, 11 pages, 2017.

[37] A. Galarneau, F. Villemot, J. Rodriguez, F. Fajula, and B. Coasne, "Validity of the t-plot method to assess microporosity in hierarchical micro/mesoporous materials," *Langmuir*, vol. 30, no. 44, pp. 13266–13274, 2014.

[38] M. Niwa and N. Katada, "New method for the temperature-programmed desorption (TPD) of ammonia experiment for characterization of zeolite acidity: a review," *Chemical Record*, vol. 13, no. 5, pp. 432–455, 2013.

[39] P. Tian, Y. Wei, M. Ye, and Z. Liu, "Methanol to olefins (MTO): from fundamentals to commercialization," *ACS Catalysis*, vol. 5, no. 3, pp. 1922–1938, 2015.

[40] Y. Li, Y. Huang, J. Guo et al., "Hierarchical SAPO-34/18 zeolite with low acid site density for converting methanol to olefins," *Catalysis Today*, vol. 233, pp. 2–7, 2014.

[41] J. Kim, M. Choi, and R. Ryoo, "Effect of mesoporosity against the deactivation of MFI zeolite catalyst during the methanol-to-hydrocarbon conversion process," *Journal of Catalysis*, vol. 269, no. 1, pp. 219–228, 2010.

[42] M. Migliori, E. Catizzone, A. Aloise et al., "New insights about coke deposition in methanol-to-DME reaction over MOR-, MFI- and FER-type zeolites," *Journal of Industrial and Engineering Chemistry*, vol. 68, pp. 196–208, 2018.